Engineering and Technology Journal

Analytical Solution for the Static Bending Elastic Analysis of Thick Rectangular Plate Structures Using 3-D Plate Theory

Festus C. Onyeka[a*] ID **, Chidobere D. Nwa-David[b]** ID **, Thompsom E. Edozie[c]**

[a] Civil Engineering Dept, Faculty of Engineering, Edo State University, Edo State, Nigeria.
[b]Civil Engineering Dept, Faculty of Engineering, Michael Okpara University of Agriculture, Umudike, Abia State, Nigeria
[c]Civil Engineering Department, Faculty of Engineering, University of Nigeria, Enugu State, Nigeria
*Corresponding author Email: edozie.okeke@unn.edu.ng

HIGHLIGHTS

- Formulation of the energy equation.
- Derivation of the exact displacement function
- Bending and stress analysis of plate.

ARTICLE INFO

ABSTRACT

In the current work, an analytical solution for static bending analysis of the thick rectangular plate structure was obtained using three-dimensional plate theory. First, the energy equation was formulated from the static elastic principles and transformed into a compatibility equation through general variation to get the slope and deflection relationship. The solution of the compatibility equation gave rise to the exact polynomial deflection function. In contrast, the coefficient of deflection and shear deformation of the plate was obtained from the governing equation through the direct variation method. These solutions were used to obtain the characteristic expression for analyzing the displacement and stresses of a rectangular plate. This formula was used for the solution of the bending problem of rectangular plate support conditions of two clamped edges, one free edge, and a simply-supported edge (CCFS). The result of the deflection and stresses decreases as the span-thickness ratio increases. More so, the aspect ratio effect of the shear stress of isotropic plates is investigated and discussed after a comparative analysis between the present work and previous studies. The result shows that the present study differs with RPT) of assumed deflection by 2.7%, whereas exact 2-D RPT by 1.9%. This shows the efficacy of the exact 3-D plate theory for rectangular plate analysis under CCFS support and loading condition.

1. Introduction

As Plates are solids with three-dimensional structural components whose thickness is small compared with the large parallel planer surfaces [1]. Plates have sustained the attention of scholars and mostly engineers with their varied applications in the construction of ship hull and decks, railways, spacecraft panels, aircraft wings, floors, slabs, and building roofs [2-4]; because of their distinguishing and advantageous properties such as lightweight, high strength, load resistance and cost benefits [5].

The application of plates is influenced by their shapes, material composition, support conditions, and weight. The plates could either be triangular, circular, or rectangular in shape. Based on material composition, they can be homogeneous, heterogeneous, anisotropic, orthotropic, or isotropic. As regards their edge conditions, the plates could be simpler-supported, free, or clamped [6]. Plates are either thin, moderately thick, or thick considering their weight [7, 8]. In [9], plates with a span-to-depth ratio of less or equal to ten are considered thick plates, those greater than or equal to forty-five are considered thin plates, while those whose ratio lies between ten and forty are seen as moderately thick plates.

Research interests in thick plates have magnified due to their better tailor ability, low density, high strength to weight, excellent corrosion resistance, high stiffness to weight, and extreme fatigue strength [10]. The behavior of thick plates can be investigated through vibration, buckling, and bending analysis [11]. This study considers the bending behavior of the thick isotropic rectangular plate. Bending is the deformation of a plate towards its surface perpendicularly with the influence of moments and external forces [12]. Plate failure occurs when deformations grow beyond the critical applied load [13]. The stability and safety of plates depend on the value of this critical load, which becomes a major concern in the investigation of plate structures. Since an exact solution for the bending properties of thick plates is essential, this research is valid.

The classical plate theory (CPT) [14] cannot address the bending of thick plates due to its inability to consider the effect of shear deformation [15]. The refined plate theories (RPT) consist of the first order shear deformation plate theory (FSDT), exponential shear deformation theory (ESDT) [16], the trigonometric shear deformation theory (TSDT) [17], polynomial shear deformation theory (PSDT) [18] and the higher-order shear deformation plate theories (HSDT). RPT is employed to analyze thick plates as the limitation of CPT is handled in FSDT using the shear correction factor [19, 20], while in HSDT, varying functions are used to the changes in transversal shear stress at the plate surfaces [21]. However, the normal strain and stress in the thickness axis of the plate are neglected in 2-D theories. On the other hand, applying 3-D theories makes it a reality to get an exact bending result. Hence the need for this study is amplified.

The deformations of thick plates can be analyzed numerically or analytically. The numerical methods offer approximate solutions. This approach includes a boundary element, finite difference, weighted residual, finite element, Bubnov-Galerkin, Collocation, and Variational Galerkin, Ritz, or Kantorovich methods. Plate problems have been analyzed numerically in [22 - 24]. Analytical methods provide closed-form solutions as they satisfy the governing equations on the plate's boundaries and in all the points on the plate surface. The Levy series, Navier series, Eigen expansion methods, and the integral transforms method are considered analytical techniques [25].

This study analytically applies 3-D plate theory with an energy approach and trigonometric function to obtain an exact bending solution of thick rectangular isotropic plate material under CCFS [C-Clamped; F-Free; S-Simply Supported] support conditions subjected to a uniformly distributed loading.

Ghugal and Gajbhiye [26] analyzed the bending of simply supported plates with HSDT and the virtual work principle. The shear and strain deformation effects were considered in their study without applying the shear correction factor linked with FSDTs. Although the analytical approach was used, the 3-D plate theory was not employed, and their study couldn't cover plates with CCFS edge conditions.

The displacements and stresses of an all-around clamped rectangular thick plate were obtained by Ibearugbulem et al. [27] with the variational method and polynomial deflection function. The results obtained satisfied the zero shear-stress state at the plate surfaces. Trigonometric functions and three-dimensional plate theory were absent in their analysis. Their study did not address CCFS plates.

The moments, shear forces, displacements, deflections, and deformation rotations at the arbitrary points of thick plates were investigated by Onyeka et al. [28] using RPT and polynomial function. Their bending analysis neglected the stress and strain in the thickness direction. The 3-D theory was not represented in their study. Neither was a trigonometric function considered. CCFS plates were not addressed.

Onyeka et al. [4] applied a modified deformation theory using a polynomial displacement function to determine an isotropic plate's lateral critical additional load. However, the authors failed to consider shear deformation along the direction of the thickness axis as well as the deflection of the plate. In addition, trigonometric shape function and CCFS plates were not covered.

RPT based on HSDT with polynomial shape function and general variational method was employed by Onyeka and Okeke [29] to address the bending traits of thick plates. They actually derived the displacement function from the principle of elasticity, but their solutions were not exact since the stresses along the thickness axis were ignored. There was no consideration for 3-D theory or trigonometric function. As a result, they failed to cover plates with the CCFS edge condition.

Ibearugbulem et al. [30] made a three-dimensional evaluation of the bending of simply supported thick plates by considering the six stress element in their analysis. Meanwhile, an assumed polynomial displacement function was used in their work rather than derived from the governing equation analytically, thereby making their final solutions inexact. Also, their analysis did not consider thick plates with the CCFS boundary condition.

Onyeka and Mama [31] used the 3-D plate theory and trigonometric shape functions with a direct variational energy method to analyze thick plates that are simply supported on all edges under a uniformly distributed load. Their work produced an exact shape function of the plate but could not address CCFS thick plate boundary condition.

The consideration that the normal stress and strain along the plate's thickness axis are negligible mars the consistency of refined plate theories, hence they are seen as 2-D plate theories. However, plates are three-dimensional elements, and 3-D plate theory should be employed in its analysis. Not much has been done by scholars in 3-D plate theory in the bending analysis of thick rectangular plates, and this gap is worth filling; to ensure the safety of plate structures in the construction industry. This study is limited to uniformly distributed load formulation as there is no available literature to validate the study with the type of load configuration (concentrated load, varying load, etc.).

Compared with previous works, the distinctiveness of this work is seen in its exact three-dimensional analytical approach, the plate support conditions, and the type of shape functions. This study focuses on the static bending behavior of thick plates with support conditions of two clamped edges, one free edge, and a simply-supported edge (CCFS) using three-dimensional plate theory with trigonometric displacement function to obtain the exact bending solution of a rectangular plate under such boundary condition. The proposed model can be applied confidently in analyzing any type of plate (thin, moderately thick, and thick plates) subjected to uniformly distributed loading since its formulation is based on exact three-dimensional theory.

2. Theoretical Section

2.1 Kinematics Relationship

As shown in Figure 1, the spatial dimensions of the plate along x, y, and z-axes are a, b and t, respectively. Therefore, the displacement field, which includes the displacements along x, y, and z-axes: u, v, and w, are obtained assuming that the x-z section and y-z section, which are initially normal to the x-y plane before bending, go off normal to the x-y plane after bending of the plate (see Figure 1).
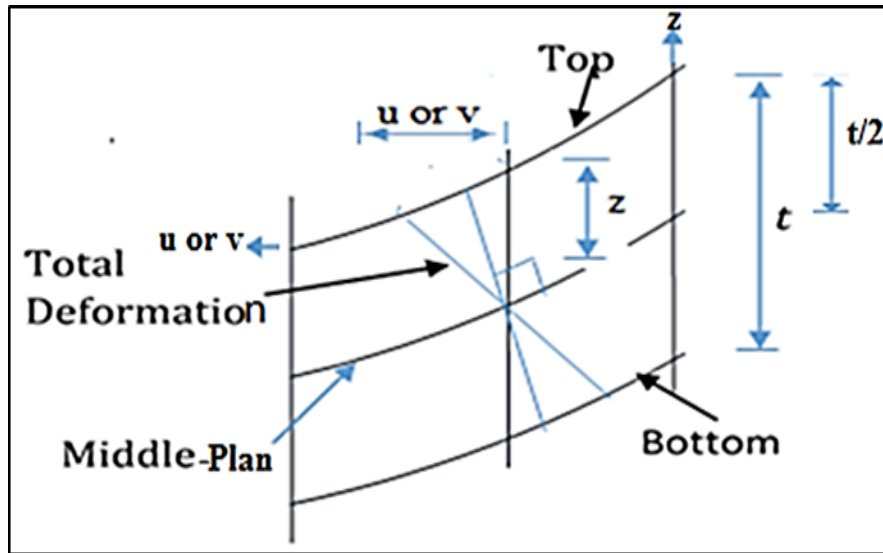
Figure 1: Displacement of x-z (or y-z) section after bending [2]

Considering the assumption of the thick plate, as stated in section 3.1, the deformation diagram in Figure 1 can be resolved using trigonometric relations for small angles. The algebraic relationship between the slope along the x-axis and y becomes:

$$\theta_{sx} = \frac{\partial u}{\partial z} \tag{1}$$

$$\theta_{sy} = \frac{\partial v}{\partial z} \tag{2}$$

The non-dimensional form of the in-plane displacement along the x and y axis gotten from the Figure 1 using trigonometric relations and can be written as presented in Equations (3) and (4) gives:

$$u = ts.\theta_{sx} \tag{3}$$

$$v = ts.\theta_{sy} \tag{4}$$

Thus, the three non-dimensional coordinates of normal strain components were derived using strain-displacement expression according to Hooke's law and presented in Equation (5) - (7):

$$\varepsilon_x = \frac{1}{a}.\frac{\partial u}{\partial R} \tag{5}$$

$$\varepsilon_y = \frac{1}{a\beta}.\frac{\partial v}{\partial Q} \tag{6}$$

$$\varepsilon_z = \frac{1}{t}.\frac{\partial w}{\partial s} \tag{7}$$

Where:
u is the inplane displacement along the x-axis of the plate
v is the inplane displacement along the x-axis of the plate
w is the out-of-plane displacement along the z-axis of the plate
R *is the* $\mathrm{non-dimensional\ parameters\ of\ the\ x-axis}$
Q *is the* $\mathrm{non-dimensional\ parameters\ of\ the\ y-axis}$
s *is the* $\mathrm{non-dimensional\ parameters\ of\ the\ z-axis}$

Similarly, the three non-dimensional coordinates shear strain components were derived using strain-displacement expression according to Hooke's law and presented in Equation (8) - (10):

$$\gamma_{xy} = \frac{1}{a\beta}.\frac{\partial u}{\partial Q} + \frac{1}{a}.\frac{\partial v}{\partial R} \tag{8}$$

$$\gamma_{xz} = \frac{1}{t}.\frac{\partial u}{\partial s} + \frac{1}{a}.\frac{\partial w}{\partial R} \tag{9}$$

$$\gamma_{yz} = \frac{1}{t} \cdot \frac{\partial v}{\partial s} + \frac{1}{a\beta} \cdot \frac{\partial w}{\partial Q} \tag{10}$$

Where:

$$x = aR \tag{11a}$$

$$y = bQ \tag{11b}$$

$$\beta = b/a \tag{12}$$

2.2 Constitutive Relations

According to Hooke's law, the 3-D constitutive relation was obtained, and the result is separated into two equations, one for the normal stress- normal strains relation:

$$\begin{bmatrix} \sigma_x \\ \sigma_y \\ \sigma_z \end{bmatrix} = \frac{E}{(1+\mu)(1-2\mu)} \begin{bmatrix} (1-\mu) & \mu & \mu \\ \mu & (1-\mu) & \mu \\ \mu & \mu & (1-\mu) \end{bmatrix} \begin{bmatrix} \varepsilon_x \\ \varepsilon_y \\ \varepsilon_z \end{bmatrix} \tag{13}$$

And the other is the for shear stress- shear strains relation:

$$\begin{bmatrix} \tau_{xz} \\ \tau_{yz} \\ \tau_{xy} \end{bmatrix} = \frac{E}{2(1+\mu)} \begin{bmatrix} \gamma_{xz} \\ \gamma_{yz} \\ \gamma_{xy} \end{bmatrix} \tag{14}$$

The three normal stress components were obtained by substituting Equations 3 to 7 into Equation 13 and simplifying the outcome as:

$$\sigma_x = \frac{E}{(1+\mu)(1-2\mu)} \left[(1-\mu) \frac{ts}{a} \cdot \frac{\partial \theta_{sx}}{\partial R} + \mu \frac{ts}{a\beta} \cdot \frac{\partial \theta_{sy}}{\partial Q} + \mu \frac{1}{t} \cdot \frac{\partial w}{\partial S} \right] \tag{15}$$

$$\sigma_y = \frac{E}{(1+\mu)(1-2\mu)} \left[\mu ts \cdot \frac{\partial \theta_{sx}}{a \partial R} + \frac{(1-\mu)ts}{a\beta} \cdot \frac{\partial \theta_{sy}}{\partial Q} + \frac{\mu}{t} \cdot \frac{\partial w}{\partial S} \right] \tag{16}$$

$$\sigma_z = \frac{E}{(1+\mu)(1-2\mu)} \left[\mu ts \cdot \frac{\partial \theta_{sx}}{a \partial R} + \frac{\mu ts}{a\beta} \cdot \frac{\partial \theta_{sy}}{\partial Q} + \frac{(1-\mu)}{t} \cdot \frac{\partial w}{\partial S} \right] \tag{17}$$

The three shear stress components were obtained by substituting Equations 8 to 10 into Equation 14 and simplifying the outcome as:

$$\tau_{xy} = \frac{E(1-2\mu)}{(1+\mu)(1-2\mu)} \cdot \left[\frac{ts}{2a\beta} \frac{\partial \theta_{sx}}{\partial Q} + \frac{ts \partial \theta_{sy}}{2a \partial R} \right] \tag{18}$$

$$\tau_{xz} = \frac{(1-2\mu)E}{(1+\mu)(1-2\mu)} \cdot \left[\frac{\theta_{sx}}{2} + \frac{1}{2a} \frac{\partial w}{\partial R} \right] \tag{19}$$

$$\tau_{yz} = \frac{(1-2\mu)E}{(1+\mu)(1-2\mu)} \cdot \left[\frac{\theta_{sy}}{2} + \frac{1}{2a\beta} \frac{\partial w}{\partial Q} \right] \tag{20}$$

2.3 Strain Energy

Strain energy is defined as the average of the product of stress and strain indefinitely summed up within the spatial domain of the body. For a unit length of the plate material (integration boundary of 0-1), the strain energy equation is expressed mathematically as:

$$U = \frac{abt}{2} \int_0^1 \int_0^1 \int_{-0.5}^{0.5} \left(\sigma_x \varepsilon_x + \sigma_y \varepsilon_y + \sigma_z \varepsilon_z + \tau_{xy} \gamma_{xy} + \tau_{xz} \gamma_{xz} + \tau_{yz} \gamma_{yz} \right) dR\, dQ\, dS \tag{21}$$

In the mid-plane of the plate, the deflection occurs (integration boundary of 0-0.5). Thus, substituting the values of stresses and strains into Equation 21 and integrating its dot product with respect to *dS* gives:

$$\text{U} = \frac{D^* ab}{2a^2} \int_0^1 \int_0^1 \left[(1-\mu)\left(\frac{\partial \theta_{sx}}{\partial R}\right)^2 + \frac{1}{\beta}\frac{\partial \theta_{sx}}{\partial R}\cdot\frac{\partial \theta_{sy}}{\partial Q} + \frac{(1-\mu)}{\beta^2}\left(\frac{\partial \theta_{sy}}{\partial Q}\right)^2 + \frac{(1-2\mu)}{2\beta^2}\left(\frac{\partial \theta_{sx}}{\partial Q}\right)^2 + \frac{(1-2\mu)}{2}\left(\frac{\partial \theta_{sy}}{\partial R}\right)^2 + \right.$$
$$\frac{12.(1-2\mu)}{2t^2}\left(a^2\theta_{sx}{}^2 + a^2\theta_{sy}{}^2 + \left(\frac{\partial w}{\partial R}\right)^2 + \frac{1}{\beta^2}\left(\frac{\partial w}{\partial Q}\right)^2 + 2a.\,\theta_{sx}\frac{\partial w}{\partial R} + \frac{2a.\theta_{sy}}{\beta}\frac{\partial w}{\partial Q}\right) + 0 * 2\frac{\mu a}{t^2}\cdot\left(\frac{\partial \theta_{sx}}{\partial R}\cdot\frac{\partial w}{\partial S} + \right.$$
$$\left. \frac{1}{\beta}\cdot\frac{\partial \theta_{sy}}{\partial Q}\cdot\frac{\partial w}{\partial S}\right) + \frac{(1-\mu)a^2}{t^4}\left(\frac{\partial w}{\partial S}\right)^2 \right] \text{dR dQ} \tag{22}$$

Where:

$$D^* = \frac{Et^3}{12(1+\mu)(1-2\mu)} \tag{23}$$

2.4 Energy Equation Formulation

Total Energy Expression be the algebraic summation of strain energy (U) and external work (V). That is:

$$\prod = \text{U} - \text{V} \tag{24}$$

$$V = abqA_1 \int_0^1 \int_0^1 h\, dR\, dQ \tag{25}$$

Where

$A_1 = $ coefficient of deflection of the plate

Substituting Equations 22 and 25 into Equation 24 gives:

$$\prod = \frac{D^* ab}{2a^2} \int_0^1 \int_0^1 \left[(1-\mu)\left(\frac{\partial \theta_{sx}}{\partial R}\right)^2 + \frac{1}{\beta}\frac{\partial \theta_{sx}}{\partial R}\cdot\frac{\partial \theta_{sy}}{\partial Q} + \frac{(1-\mu)}{\beta^2}\left(\frac{\partial \theta_{sy}}{\partial Q}\right)^2 + \frac{(1-2\mu)}{2\beta^2}\left(\frac{\partial \theta_{sx}}{\partial Q}\right)^2 + \frac{(1-2\mu)}{2}\left(\frac{\partial \theta_{sy}}{\partial R}\right)^2 + \right.$$
$$\frac{6(1-2\mu)}{t^2}\left(a^2\theta_{sx}{}^2 + a^2\theta_{sy}{}^2 + \left(\frac{\partial w}{\partial R}\right)^2 + \frac{1}{\beta^2}\left(\frac{\partial w}{\partial Q}\right)^2 + 2a.\,\theta_{sx}\frac{\partial w}{\partial R} + \frac{2a.\theta_{sy}}{\beta}\frac{\partial w}{\partial Q}\right) + \frac{(1-\mu)a^2}{t^4}\left(\frac{\partial w}{\partial S}\right)^2 \right] dR\, dQ -$$
$$\int_0^1 \int_0^1 abqhA_1 \partial R \partial Q \tag{26}$$

2.5 Governing Equation

The solution of the governing equation in trigonometric form is obtained in line with the work of Onyeka *et al.* [28] by minimizing the total potential energy functional with respect to deflection to give the exact deflection equation, shear deformation rotation in the x-axis, and shear deformation rotation in y-axis as presented in Equation 27, 28 and 29 respectively:

$$w = \Delta_0.\,[a_0 + a_1 R + a_2 Cos\,(c_1 R) + a_3 Sin\,(c_1 R)].\,b_0 + b_1 Q + b_2 Cos\,(c_1 Q) + b_3 Sin\,(c_1 Q) \tag{27}$$

$$\theta_{sx} = \frac{c}{a}.\,\Delta_0.\,[a_1 + a_2 c_1 Sin\,(c_1 R) + a_3 c_1 Cos\,(c_1 R)].\,[b_0 + b_1 Q + b_2 Cos\,(c_1 Q) + b_3 Sin\,(c_1 Q)] \tag{28}$$

$$\theta_{sy} = \frac{c}{a\beta}.\,\Delta_0.\,[a_0 + a_1 R + a_2 Cos\,(c_1 R) + a_3 Sin\,(c_1 R)].\,[b_1 + b_2 c_1 Sin\,(c_1 Q) + b_3 c_1 Cos\,(c_1 Q)] \tag{29}$$

Let:

$$w = A_1.\,h \tag{30}$$

$$\theta_{sx} = \frac{A_2}{a}.\,\frac{\partial h}{\partial R} \tag{31}$$

$$\theta_{sy} = \frac{A_3}{a\beta}.\,\frac{\partial h}{\partial Q} \tag{32}$$

Where: $A_2 = $ coefficient of shear deformation along the x-axis of the plate; $A_3 = $ coefficient of shear deformation along the y-axis of the plate

Substituting Equations 30, 31, and 32 into 26 gives:

$$\prod = \frac{D^* ab}{2a^4}\left[(1-\mu)A_2{}^2 k_x + \frac{1}{\beta^2}\left[A_2.\,A_3 + \frac{(1-2\mu)A_2{}^2}{2} + \frac{(1-2\mu)A_3{}^2}{2}\right] k_{xy} + \frac{(1-\mu)A_3{}^2}{\beta^4}k_y + \right.$$
$$6(1-2\mu)\left(\frac{a}{t}\right)^2\left([A_2{}^2 + A_1{}^2 + 2A_1 A_2].\,k_z + \frac{1}{\beta^2}.\,[A_3{}^2 + A_1{}^2 + 2A_1 A_3].\,k_{2z}\right) - \frac{2qa^4 k_h A_1}{D^*}\right] \tag{33}$$

Minimizing Equation 33 with respect to A_2 gives:

$$\frac{\partial \Pi}{\partial A_2} = (1-\mu)A_2 k_x + \frac{1}{2\beta^2}[A_3 + A_2(1-2\mu)]k_{xy} + 6(1-2\mu)\left(\frac{a}{t}\right)^2 [A_2 + A_1].k_z = 0 \quad (34)$$

Minimizing Equation 33 with respect to A_3 gives:

$$\frac{\partial \Pi}{\partial A_3} = \frac{(1-\mu)A_3}{\beta^4} k_y + \frac{1}{2\beta^2}[A_2 + A_3(1-2\mu)]k_{xy} + \frac{6}{\beta^2}(1-2\mu)\left(\frac{a}{t}\right)^2 ([A_3 + A_1].k_{2z}) = 0 \quad (35)$$

Rewriting Equations 34 and 35 gives:

$$\left[(1-\mu)k_x + \frac{1}{2\beta^2}(1-2\mu)k_{xy} + 6(1-2\mu)\left(\frac{a}{t}\right)^2 k_z\right]A_2 + \left[\frac{1}{2\beta^2}k_{xy}\right]A_3 = \left[-6(1-2\mu)\left(\frac{a}{t}\right)^2 k_z\right]A_1 \quad (36)$$

$$\left[\frac{1}{2\beta^2}k_{xy}\right]A_2 + \left[\frac{(1-\mu)}{\beta^4}k_y + \frac{1}{2\beta^2}(1-2\mu)k_{xy} + \frac{6}{\beta^2}(1-2\mu)\left(\frac{a}{t}\right)^2 k_{2z}\right]A_3 = \left[-\frac{6}{\beta^2}(1-2\mu)\left(\frac{a}{t}\right)^2 k_Q\right]A_1 \quad (37)$$

Solving Equations 36 and 37 simultaneously gives:

$$A_2 = MA_1 \qquad (38)$$

$$A_3 = NA_1 \qquad (39)$$

Let:

$$M = \frac{(r_{12}r_{23} - r_{13}r_{22})}{(r_{12}r_{12} - r_{11}r_{22})} \qquad (40)$$

$$N = \frac{(r_{12}r_{13} - r_{11}r_{23})}{(r_{12}r_{12} - r_{11}r_{22})} \qquad (41)$$

Where:

$$r_{11} = (1-\mu)k_x + \frac{1}{2\beta^2}(1-2\mu)k_{xy} + 6(1-2\mu)\left(\frac{a}{t}\right)^2 k_z \qquad (42)$$

$$r_{22} = \frac{(1-\mu)}{\beta^4}k_y + \frac{1}{2\beta^2}(1-2\mu)k_{xy} + \frac{6}{\beta^2}(1-2\mu)\left(\frac{a}{t}\right)^2 k_{2z} \qquad (43)$$

$$r_{12} = r_{21} = \frac{1}{2\beta^2}k_{xy}; \; r_{13} = -6(1-2\mu)\left(\frac{a}{t}\right)^2 k_z; \; r_{23} = r_{32} = -\frac{6}{\beta^2}(1-2\mu)\left(\frac{a}{t}\right)^2 k_{2z} \quad (44)$$

Minimizing Equation 33 with respect to A_1 gives:

$$\frac{\partial \Pi}{\partial A_1} = \frac{D^* ab}{2a^4}\left[6(1-2\mu)\left(\frac{a}{t}\right)^2 \left([2A_1 + 2A_2].k_z + \frac{1}{\beta^2}.[2A_1 + 2A_3].k_{2z}\right) - \frac{2qa^4 k_h}{D^*}\right] = 0 \quad (45)$$

That is:

$$6(1-2\mu)\left(\frac{a}{t}\right)^2 \left([A_1 + UA_1].k_z + \frac{1}{\beta^2}.[A_1 + VA_1].k_{2z}\right) - \frac{qa^4 k_h}{D^*} = 0 \quad (46)$$

Factorizing Equations (46) and simplifying gives:

$$6(1-2\mu)\left(\frac{a}{t}\right)^2 A_1 \left([1 + U].k_z + \frac{1}{\beta^2}.[1 + V].k_{2z}\right) = \frac{qa^4 k_h}{D^*} \qquad (47)$$

$$TA_1 = \frac{qa^4 k_h}{D^*} \qquad (48)$$

$$A_1 = \frac{qa^4}{D^*}\left(\frac{k_h}{T}\right) \qquad (49)$$

Where:

$$T = 6(1 - 2\mu)\left(\frac{a}{t}\right)^2 * \left([1 + U].k_z + \frac{1}{\beta^2}.[1 + V].k_{2z}\right) \tag{50}$$

2.6 Exact Displacement and Stress Equation of the Plate

The numerical analysis of a thick rectangular plate whose Poisson's ratio is 0.3 under CCFS boundary conditions, as shown in Figure 2, and carrying uniformly distributed load (including self-weight) is presented. An exact trigonometric function was obtained in Equation 27 and applied here to get the actual values of the shape functions, coefficients of deflection, and shear deformation rotations at the x and y-axis of the plate.
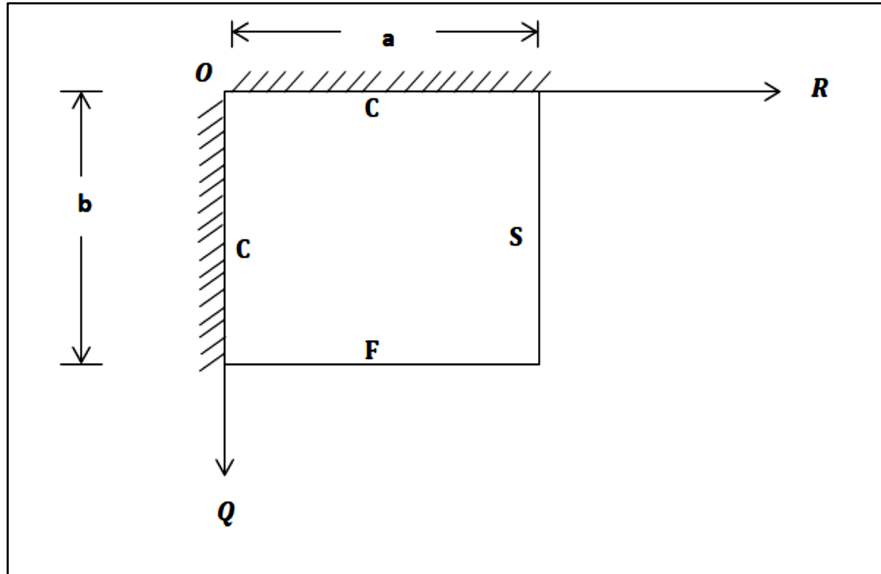
Figure 2: CCFS rectangular plate

The trigonometric deflection $w\ (x, y)$ functions after satisfying the boundary conditions of the plate in Figure 2 (see [6]) is:

$$w = A_1(\ g_1 - g_1 R - g_1 Cos\ g_1 R + Sin\ g_1 R).\left(Cos\frac{\pi Q}{2} - 1\right) \tag{51}$$

Substituting Equations (31), (32), (38), (39) and (49) into Equation (1) gives the in-plane displacement along x-axis as:

$$u = ts.\frac{M}{a}.\frac{qa^4}{D^*}\left(\frac{k_h}{T}\right)\frac{\partial h}{\partial R} \tag{52}$$

Substituting Equations (31), (32), (38), (39), and (49) into Equation (2) gives the in-plane displacement along the y-axis:

$$v = ts.\frac{N}{a\beta}.\frac{qa^4}{D^*}\left(\frac{k_h}{T}\right)\frac{\partial h}{\partial Q} \tag{53}$$

Substitute Equation (49) into Equation (51), which gives the deflection equation of the plate as:

$$w = (\ g_1 - g_1 R - g_1 Cos\ g_1 R + Sin\ g_1 R).\left(Cos\frac{\pi Q}{2} - 1\right).\frac{qa^4}{D^*}\left(\frac{k_h}{T}\right) \tag{54}$$

Substituting Equations (31), (32), (38), (39), and (49) into Equation (15) – (17), where appropriate, gives the three normal stress at the x, y, and z axis in Equations (55), (56) and (57) respectively:

$$\sigma_x = \frac{E}{(1+\mu)(1-2\mu)}\left[(1-\mu)\frac{ts}{a}.\frac{\partial^2 h}{\partial R^2}A_2 + \mu\frac{ts}{a\beta}.\frac{\partial^2 h}{\partial Q^2}A_3 + \mu\frac{1}{t}.\frac{qa^4}{D^*}\left(\frac{k_h}{T}\right)\frac{\partial h}{\partial S}A_1\right] \tag{55}$$

$$\sigma_y = \frac{E}{(1+\mu)(1-2\mu)}\left[\frac{\mu ts}{a}.\frac{\partial^2 h}{\partial R^2}A_2 + \frac{(1-\mu)ts}{a\beta}.\frac{\partial^2 h}{\partial Q^2}A_2 + \frac{\mu}{t}.\frac{qa^4}{D^*}\left(\frac{k_h}{T}\right)\frac{\partial h}{\partial S}A_1\right] \tag{56}$$

$$\sigma_z = \frac{E}{(1+\mu)(1-2\mu)}\left[\frac{\mu ts}{a}.\frac{\partial^2 h}{\partial R^2}A_2 + \frac{\mu ts}{a\beta}.\frac{\partial^2 h}{\partial Q^2}A_3 + \frac{(1-\mu)}{t}.\frac{qa^4}{D^*}\left(\frac{k_h}{T}\right)\frac{\partial h}{\partial S}A_4\right] \tag{57}$$

Substituting Equations (31), (32), (38), (39), and (49) into Equation (18) – (20), where appropriate, gives the three normal stress at the x, y, and z axis in Equations (58), (59) and (60) respectively:

$$\tau_{xy} = \frac{E(1-2\mu)}{(1+\mu)(1-2\mu)} \cdot \left[\frac{ts}{2a\beta} \cdot \frac{\partial^2}{\partial R\,\partial Q} A_2 + \frac{ts}{2a} \cdot \frac{\partial^2}{\partial R\,\partial Q} A_3 \right] \tag{58}$$

$$\tau_{xz} = \frac{(1-2\mu)E}{(1+\mu)(1-2\mu)} \cdot \left[\frac{A_2}{2a} \frac{\partial h}{\partial R} + \frac{1}{2a} \cdot \frac{qa^4}{D^*} \left(\frac{k_h}{T} \right) \frac{\partial h}{\partial R} \right] \tag{59}$$

$$\tau_{yz} = \frac{(1-2\mu)E}{(1+\mu)(1-2\mu)} \cdot \left[\frac{A_2}{2a} \frac{\partial h}{\partial Q} + \frac{1}{2a\beta} \cdot \frac{qa^4}{D^*} \left(\frac{k_h}{T} \right) \frac{\partial h}{\partial Q} \right] \tag{60}$$

3. Results and Discussion

The numerical results of non-dimensional displacements (u, v, and w) and the stresses perpendicular to the x, y and z axis (σ_x, σ_y & σ_z) and shear stresses along the x-y, x-z, and y-z (τ_{xy}, τ_{xz} and τ_{yz}) of a 3-D rectangular isotropic plate material subjected to uniformly distributed load was obtained using the established exact trigonometric displacement function to analyze the effect of the aspect ratio of the bending characteristics of the plate. The rectangular plate was clamped at the first and second edges, freely and simply supported at the third and fourth edges, respectively. An aspect ratio of 1 and 2 was considered in this work, while the span-thickness ratio range of 4, 5, 10, 15, 20, 50, 100, and CPT was evaluated. This ratio range was used as they appeared to be the points where significant plate deformation changes were noticed. The comparative numerical analysis was presented to show the disparities between the present study and the literature under review to show the effect of the span-thickness ratio on the deflection of the rectangular plate at varying aspect ratios. Table 1 shows the results of the percentage difference evaluation performed for the span-thickness ratio of 4, 5, 30, 50, and 100 only. Hence, for the purpose of the result discussion, only the aspect ratio of 1.5 was used to measure the variation between the present work and past studies percentage-wise.

The result of the comparative analysis performed in Table 1 showed the disparity between different theories used in the plate analysis, especially as it concerns thick plates. This theory includes 2-D RPT with assumed deflection, 2-D RPT with derived deflection function, and 3-D theory of elasticity. A percentage difference evaluation was adopted, as presented in Table 1, to compare and show the validity of the derived relationships in the deflection analysis. This proved that the plate is a typical three-dimensional element and required a 3-D theory of elasticity for a more accurate and reliable result. The average percentage difference analysis between the present study and the work of Gwarah [32] and Onyeka *et al.* [33] at an aspect ratio of 1.5 is 2.26% and 3.26%, respectively. The small difference between the work of Onyeka *et al.* [33] when compared with the present work (exact 3-D theory) is quite expected. They used RPT with a derived deflection function from the elasticity principle, which makes their solution close-form, whereas Gwarah [32] used an assumed deflection function which gives a higher difference with an exact 3-D theory of elasticity (Present study) when compared to the work of Onyeka *et al.* [33]. The overall percentage difference between the present study and RPT [32 and 33] is 2.8%. The small difference showed that at about 97% significant, both models are the same and, thus, depict the validity of the present models in the rectangular plate analysis under CCFS support and loading and condition.

Table 1: Comparative deflection analysis for the square plate at varying span-thickness ratio (β = a/t) between the present study and past studies

$\beta = \dfrac{a}{t}$	Present Study	Onyeka *et al.* [33]	Percentage difference (%)	Gwarah [32]	Percentage difference (%)
4	0.0053	0.0054	1.887	0.0053	0.000
5	0.0047	0.0048	2.128	0.0048	2.128
10	0.0038	0.0040	5.263	0.0041	7.895
30	0.0038	0.0039	2.632	0.0039	2.632
50	0.0038	0.0039	2.632	0.0039	2.632
100	0.0037	0.0038	2.703	0.0039	5.405
CPT	0.0037	0.0038	2.027	0.0039	5.405

The non-dimensional result in Table 2 shows that as the span-thickness ratio of the plate increase, the in-plane displacement along the x and y axis (u and v) increases too, whereas the deflection (w) which occurs at the plate due to the applied load decrease with increases in the value of the span-thickness ratio of the plate. On the other hand, the stress perpendicular to the x, y, and z-axis (σ_x, σ_y & σ_z) decreases as the span-depth ratio of the plate increases. Meanwhile, the increase in the span-thickness ratio of the plate increases the value of shear stress along the x-y (τ_{xy}) while the span-depth ratio causes a decrease in the value shear stress along the x-z and y-z plane (τ_{xz} & τ_{yz}). These decreases continue until the plate structure deflects beyond the elastic yield stress. Hence, failure occurs.

Table 2 shows that at a span-depth ratio between 4 and 15, deflection values vary between 0.0044 and 0.0031. At a span-depth ratio between 30, the value of deflection maintains a constant value of 0.0030. More so, at the span-depth ratio of 30 and above, a constant value of 0.0030 is noticed. This value is equal to the value of the CPT. This is quite expected since we assumed in CPT analyses that at span-thickness ratios of 100 and above, a plate could be taken as being thin. Similarly, it can be seen that at a span-depth ratio between 4 and 15, the non-dimensional value of transverse shear stress along x-z coordinates varies between

0.0054 and 0.0002, a constant value of -0.0001, which is equal to the value of the CPT is noticed at the span-depth ratio of 30 and above. It can be deduced that the value of deflection and shear stress varies more as the plate is thicker and vary less as the span - depth increase (thinner plate) under the same loading capacity/condition. Therefore, it can be said that the plate is considered thick at a span - depth ratio below 30. The result of the numerical analysis showed that at span - depth ratio below 30, the plate can be classified as thick and beyond. It can be said that the plate can be classified as thin at the span-depth ratio of 30 and above because, at this point, the value of the span-depth ratio coincides with the value of the CPT.

The non-dimensional result in Table 2 shows that as the span-thickness ratio of the plate increase, the in-plane displacement along the x and y axis (u and v) increases too, whereas the deflection (w) which occurs at the plate due to the applied load decrease with increases in the value of the span-thickness ratio of the plate. On the other hand, the stress perpendicular to the x, y, and z-axis (σ_x, σ_y & σ_z) decreases as the span-depth ratio of the plate increases. Meanwhile, the increase in the span-thickness ratio of the plate increases the value of shear stress along the x-y plane (τ_{xy}) while the span-depth ratio causes a decrease in the value shear stress along the x-z and y-z plane (τ_{xz} & τ_{yz}). These decreases continue until the plate structure deflects beyond the elastic yield stress. Hence, failure occurs.

Table 2: The result of displacements and stresses of a CCFS aspect ratio of 1.0

$\beta = \frac{a}{t}$	w	u	v	σ_x	σ_y	σ_z	τ_{xy}	τ_{xz}	τ_{yz}
4	0.0044	-0.0019	0.2953	0.2414	0.1741	0.1682	-0.0308	0.0047	0.0311
5	0.0039	-0.0018	0.2772	2.1352	0.1636	0.1671	-0.0290	0.0029	0.0193
10	0.0032	-0.0016	0.2537	1.7728	0.1501	0.1660	-0.0267	0.0006	0.0039
15	0.0031	-0.0016	0.2495	1.7085	0.1476	0.1659	-0.0263	0.0002	0.0011
30	0.0030	-0.0016	0.2469	1.6862	0.1462	0.1658	-0.0261	-0.0001	-0.0006
50	0.0030	-0.0016	0.2464	1.6622	0.1458	0.1658	-0.0260	-0.0001	-0.0010
100	0.0030	-0.0016	0.2461	1.6588	0.1457	0.1658	-0.0260	-0.0001	-0.0011
CPT	0.0030	-0.0016	0.2461	1.6577	0.1457	0.1658	-0.0260	-0.0001	-0.0011

Table 3 shows that at a span-depth ratio between 4 and 10, deflection values vary between 0.0053 and 0.0047. At a span-depth ratio between 4 and 50, the value of deflection maintains a constant value of 0.0038. More so, at the span-depth ratio of 50 and above, a constant value of 0.0037 is noticed. This value is equal to the value of the CPT. This is quite expected since we assumed in CPT analyses that at span-thickness ratios of 100 and above, a plate could be taken as being thin. Similarly, it can be seen that at a span-depth ratio between 4 and 15, the non-dimensional value of transverse shear stress along x-z coordinates varies between 0.0054 and 0.0001, a constant value of 0.0037, which is equal to the value of the CPT is noticed at the span-depth ratio of 50 and above. It can be deduced that the value of deflection and shear stress varies more as the plate is thicker and vary less as the span - depth increase (thinner plate) under the same loading capacity/condition. Therefore, it can be said that the plate is considered thick at a span-depth ratio between 4 and 30. The result of the numerical analysis showed that the plate could be classified as thick at a span-thickness ratio of 10 and below. Therefore, the plate can be classified as moderately thick between the span-depth ratio of 10 and 50. Also, the thin plate is taken as the plate with a span-depth ratio beyond 50 because, at this point, the span-depth ratio's value coincides with the CPT value.

Table 3: Displacement and stresses of a CCFS plate aspect ratio of 1.5

$\beta = \frac{a}{t}$	w	u	v	σ_x	σ_y	σ_z	τ_{xy}	τ_{xz}	τ_{yz}
4	0.0053	-0.0024	-0.0112	0.34049	0.1501	0.3554	-0.0257	0.0054	0.0181
5	0.0047	-0.0023	-0.0106	0.32159	0.1413	0.3445	-0.0243	0.0034	0.0109
10	0.0038	-0.0021	-0.0096	0.29257	0.1276	0.3296	-0.0220	0.0003	0.0001
15	0.0038	-0.0021	-0.0096	0.29101	0.1269	0.3268	-0.0219	0.0001	-0.0005
30	0.0038	-0.0021	-0.0095	0.28966	0.1263	0.3251	-0.0218	-0.0001	-0.0010
50	0.0037	-0.0021	-0.0094	0.28933	0.1261	0.3247	-0.0217	-0.0001	-0.0011
100	0.0037	-0.0020	-0.0094	0.28909	0.1260	0.3245	-0.0217	-0.0001	-0.0012
CPT	0.0037	-0.0020	-0.0094	0.28909	0.1260	0.3245	-0.0217	-0.0001	-0.0012

Study in Table 2 and 3 shows that as the aspect ratio of the plate increase, the in-plane displacement along the x and y axis (u and v) decrease, whereas the deflection (w) which occurs in the plate due to the applied load increase with increases in the value of the span-thickness ratio of the plate. On the other hand, the stress perpendicular to the x, y, and z axis increase as the span-depth ratio of the plate increases. This implies that, as the length of the plate material increases, more stresses are induced in the plate, leading to the plate material's failure if the plate material is stretched beyond the elastic limit. This means that the failure in a plate structure is bound to occur as more stresses are induced within the plate element, which affects the performance in terms of the serviceability of the plate. Thus, caution must be taken when selecting the depth and other dimensions along the x and y coordinates of the plate to ensure the accuracy of the analysis and safety in the construction.

In summary, there are three categories of rectangular plates. The plates whose deflection and vertical shear stress do not vary much with CPT is categorized as a thin plate. Hence, the plate whose deflection and transverse shear stress varies very much from zero is categorized as a thick plate. Thus, the span-thickness ratio for these categories of rectangular plates is: Thick plate is categorized as the plate with the span to thickness ratio: $a/t \leq 15$, while the moderately thick plate is categorized as the plate with the span to thickness ratio: of $15 < a/t < 50$. Also, the thin plate is categorized as the plate with the span-to-thickness

ratio: $a/t > 50$. Thus, the present theory of stress prediction shows that the result of the displacement and stress of thin plate using the 3-D theory is the same as the CPT for the bending analysis of rectangular plate at span-depth ratio beyond 50 under the CSCS boundary condition.

4. Conclusion

The 3-D stress analysis of thick rectangular plates using 3-D elasticity theory has been investigated. The following conclusions can be drawn based on this research:

1) Trigonometric shape function predicts a close-form solution than the polynomial displacement function.
2) The present theory of stress prediction shows that the result of the displacement and stress of thin and moderately thick plates using the 3-D theory is the same at span-thickness ratio beyond 50% for the bending analysis of rectangular plates under the CSCS boundary condition.
3) Plate analysis required a 3-D analogy for a true solution, but the 2-D shear deformation theory gives an unrealistic solution.
4) The 3-D exact plate model developed in this study is variationally consistent and can be used to analyze any plate category.

Acknowledgment

Author contribution

All authors contributed equally to this work.

Funding

Data availability statement

Not applicable.

Conflicts of interest

The authors declare that there is no conflict of interest.

References

[1] F. C. Onyeka, B. O. Mama, C. D. Nwa-David, Application of variation method in three-dimensional stability analysis of rectangular plate using various exact shape functions, Niger. J. Technol., 41 (2022) 8-20. http://dx.doi.org/10.4314/njt.v41i1.2

[2] F. C. Onyeka, T. E. Okeke, C. D. Nwa-David, Static and buckling analysis of a three-dimensional (3-D) rectangular thick plates using exact polynomial displacement function, European J. Adv. Eng. Technol., 7 (2022). http://dx.doi.org/10.24018/ejeng.2022.7.2.2725

[3] F. C. Onyeka, C. D. Nwa-David, T. E. Okeke, Study on stability analysis of rectangular plates section using a three-dimensional plate theory with polynomial function, J. Eng. Res., 1 (2022) 28-37. https://dx.doi.org/10.55708/js0104004

[4] F. C. Onyeka, C. D. Nwa-David, E. E. Arinze, Structural imposed load analysis of isotropic rectangular plate carrying a uniformly distributed load using refined shear plate theory, J. Eng. Technol., 6 (2021) 414-419. http://dx.doi.org/10.46792/fuoyejet.v6i4.719

[5] F. C. Onyeka, T. E. Okeke, Application of Higher Order Shear Deformation Theory in The Analysis of Thick Rectangular Plate, nt. J. Emerg. Technol. Learn .,11 (2020) 62-67.

[6] F. C. Onyeka, B. O. Mama, C. D. Nwa-David, Analytical modelling of a three-dimensional (3-D) rectangular plate using the exact solution approach, IOSR J. Mech. Civ. Eng., 19 (2022) 76-88. http://dx.doi.org/10.9790/1684-1901017688

[7] F. C. Onyeka, B. O. Mama, T. E. Okeke, Exact three-dimensional stability analysis of plate using a direct variational energy method, Civ. Eng. J.,8 (2022) 60–80. http://dx.doi.org/10.28991/CEJ-2022-08-01-05

[8] Chandrashekhara, K. Theory of plates. University Press (India) Limited, 2001.

[9] F. C. Onyeka, F. O. Okafor, H. N. Onah, Buckling solution of a three-dimensional clamped rectangular thick plate using direct variational method, IOSR J. Mech. Civ. Eng., 18 (2021) 10-22. http://dx.doi.org/10.9790/1684-1803031022

[10] F. C. Onyeka, F. O. Okafor, H. N. Onah, Application of a new trigonometric theory in the buckling analysis of three-dimensional thick plate, Int. J. Emerg., 12 (2021) 228-240.

[11] Timoshenko, S. P., Gere J. M., Prager W. 1962. Theory of Elastic Stability, Second Edition, J. Appl. Mech. 2nd Ed., Vol. 29, Issue 1, McGraw-Hill Books Company, https://doi.org/10.1115/1.3636481

[12] P. S. Gujar, K. B. Ladhane, Bending analysis of simply supported and clamped circular plate, Int. J. Civ. Eng., 2 (2015) 45 – 51. https://doi.org/10.14445/23488352/IJCE-V2I5P112

[13] F. C. Onyeka, T. E. Okeke, Analysis of critical imposed load of plate using variational calculus, J. Adv. Sci. Eng..4 (2020) 13–23. https://doi.org/10.37121/jase.v4i1.125

[14] C. H. Aginam, C. A. Chidolue and C. A. Ezeagu, Application of Direct Variational Method in the Analysis of Isotropic thin Rectangular Plates, ARPN J. Eng. Appl. Sci., 7 (2012) 1128-1138.

[15] B. O. Mama, C. U. Nwoji, C. C. Ike, H. N. Onah, Analysis of simply supported rectangular Kirchhoff plates by the finite Fourier sine transform method, ARPN J. Eng. Appl. Sci., 4 (2017) 285 – 291. https://doi.org/10.22161/ijaers.4.3.44

[16] F. C. Onyeka, Critical lateral load analysis of rectangular plate considering shear deformation effect, Int. J. Civ. Eng., 1 (2020) 16-27. https://doi.org/10.37516/global.j.civ.eng.2020.012

[17] J. L. Mantari, A. S. Oktem,   S. C. Guedes, A new trigonometric shear deformation theory for isotropic, Laminated Composite and Sandwich Plates, Int. J. Solids Strict ., 49 (2012) 43-53. http://doi.org/10.1016/j.ijsolstr.2011.09.008

[18] O. M. Ibearugbulem, F. C. Onyeka, Moment and stress analysis solutions of clamped rectangular thick plate, 5 (2020) 531-534. https://doi.org/10.24018/ejers.2020.5.4.1898

[19] E. Reissner, The effect of transverse shear deformation on the bending of elastic plates, J. Appl. Mech., 12 (1945) A69–A77. doi:10.1115/1.4009435

[20] R. D. Mindlin, Influence of rotatory inertia and shear on flexural motions of isotropic, elastic plates, J. Appl. Mech., 18 (1951) 31–38. https://doi.org/10.1115/1.4010217

[21] F. C. Onyeka, T. E. Okeke, Elastic bending analysis exact solution of plate using alternative i refined plate theory, Niger. J. Technol., 40 (2021) 1018 –1029. http://dx.doi.org/10.4314/njt.v40i6.4

[22] N. N. Osadebe. C. C. Ike, H. N. Onah, C. U. Nwoji, F. O. Okafor, Application of Galerkin-Vlasov method to the flexural analysis of simply supported rectangular kirchhoff plates under uniform loads, Niger. J. Technol., 35 (2016) 732-738. https://doi.org/10.4314/njt.v35i4.7

[23] C. U. Nwoji, B. O. Mama, C. C. Ike, H. N. Onah H. N. Galerkin-Vlasov method for the flexural analysis of rectangular Kirchhoff plates with clamped and simply supported edges, IOSR J.. Mech. Civ. Eng., 14 (2017) 61-74. https://doi.org/10.9790/1684-1402016174

[24] C. C. Ike, Equilibrium approach in the derivation of differential equation for homogeneous isotropic Mindlin plates, Niger. J. Technol., 36 (2017) 346-350. https://doi.org/10.4314/njt.v36i2.4

[25] R. Szilard, Theories and Applications of Plates Analysis: Classical, Numerical and Engineering Methods, John Wiley and Sons Inc., (2004).

[26] Y. M. Ghugal, P. D. Gajbhiye, Bending analysis of thick isotropic plates by using 5th order shear deformation theory, J. Appl. Comput. Mech., 2 (2016) 80-95. https://doi.org/10.22055/jacm.2016.12366

[27] O. M. Ibearugbulem, J. C. Ezeh, L. O. Ettu, L. S. Gwarah, Bending analysis of rectangular thick plate using polynomial shear deformation theory, IOSR J. Compute. Eng., 8 (2018) 53-61.

[28] F. C. Onyeka, F. O. Okafor, H. N. Onah, Application of exact solution approach in the analysis of thick rectangular plate, Int. J. Appl. Eng., 14 (2019) 2043-2057.

[29] F. C. Onyeka, T. E. Okeke, Analytical solution of thick rectangular plate with clamped and free support boundary condition using polynomial shear deformation theory, Advances in Science, Adv. Sci. Technol. Eng., 6 (2021) 1427-1439. https://dx.doi.org/10.25046/aj0601162

[30] O. M. Ibearugbulem, U. C. Onwuegbuchulem, C. N. Ibearugbulem, Analytical three-dimensional bending analyses of simply supported thick rectangular plate, Int. J. Eng. Res., 3 (2021) 27–45.

[31] F. C. Onyeka, B. O. Mama, Analytical study of bending characteristics of an elastic rectangular plate using direct variational energy approach with trigonometric function, Emerge, Sci. J., 5 (2021) 916-928. http://dx.doi.org/10.28991/esj-2021-01320

[32] Gwarah, L. S. Application of Shear Deformation Theory in the Analysis of Thick Rectangular Plates using Polynomial Displacement Functions. A published PhD. Thesis Presented to the School of Civil Engineering, Federal University of Technology, Owerri, Nigeria, 2019.

[33] F. C. Onyeka and D. Osegbowa, Stress analysis of thick rectangular plate using higher order polynomial shear deformation theory, Futo J. Sci.,6 (2020) 142-161.